Fossil Record
Open Access

MUSEUM FÜR
NATURKUNDE
BERLIN

Microanatomy and growth of the mesosaurs *Stereosternum tumidum* and *Brazilosaurus sanpauloensis* (Reptilia, Parareptilia)

Nicole Klein[1], **Antoine Verrière**[2], **Heitor Sartorelli**[1], **Tanja Wintrich**[1,3], and **Jörg Fröbisch**[2,4]

[1]Abteilung Paläontologie, Institut für Geowissenschaften, Universität Bonn, Nussallee 8, 53115 Bonn, Germany
[2]Museum für Naturkunde – Leibniz-Institut für Evolutions- und Biodiversitätsforschung,
Invalidenstraße 43, 10115 Berlin, Germany
[3]Institut für Anatomie, Universitätsklinikum Bonn, Universität Bonn, Nussallee 10, 53115 Bonn, Germany
[4]Institut für Biologie, Humboldt-Universität zu Berlin, Invalidenstraße 42, 10115 Berlin, Germany

Correspondence: Nicole Klein (nklein@posteo.de)

Abstract. Histology and microanatomy of vertebrae, ribs, haemal arch, and humeri and femora of 10 individuals of *Stereosternum* and two dorsal ribs of 1 individual of *Brazilosaurus* were studied. All individuals had achieved a body length of 50 cm (equal to 65 % of the maximum known body length) or larger. All sampled bones are highly osteosclerotic due to the reduction of medullary cavities and the filling of medullary regions by endosteal bone. Calcified cartilage occurs – if at all – only locally in small clusters in the medullary regions of midshaft and in higher amounts only in non-midshaft sections of long bones and towards the medio-distal rib shaft, respectively. The primary bone tissue consists of highly organized parallel-fibred tissue and/or lamellar tissue, which is in most samples relatively lightly vascularized or even avascular. If present, vascular canals are mainly longitudinally oriented; some show a radial orientation. Simple vascular canals as well as primary osteons occur. Some of the latter are secondarily altered, i.e. widened. Remodelling of the periosteal cortex is only documented by few scattered erosion cavities and secondary osteons. The tissue is regularly stratified by lines of arrested growth (LAGs), which usually appear as double or multiple rest lines, indicating strong dependence on exogenous and endogenous factors. Because of the inhibition of periosteal remodelling the growth record is complete and no inner cycles are lost. Individuals of *Stereosternum* show a poor correlation of body size and number of growth marks, which might be the result of developmental plasticity. *Brazilosaurus* shows a highly organized, avascular lamellar tissue and a high number of regularly deposited rest lines throughout the cortex of the ribs. The medullary region in the ribs of *Brazilosaurus* is distinctly larger when compared to ribs of *Stereosternum*. However, strong osteosclerosis is obvious in both taxa, pointing to a high degree of aquatic adaption. Ribs of *Stereosternum*, *Brazilosaurus*, and *Mesosaurus* are clearly distinguishable from each other by the distribution of the periosteal and endosteal territory. Furthermore, *Brazilosaurus* differs in its growth pattern (i.e. spacing of rest lines) when compared to *Stereosternum* and *Mesosaurus*.

1 Introduction

The Permian family Mesosauridae is involved in several key events of the history of life and that of natural sciences. First of all, mesosaurs are exclusively found in early Permian black-shale and limestone deposits from both southeastern South America (the Irati Formation in southern Brazil and the Melo Formation in Uruguay) and southwestern Africa (the Whitehill Formation in Namibia and in western South Africa) (Oelofsen and Araújo, 1987). Because of this geographical distribution, which supports the theory that the two continents were once connected, mesosaurs were among the fossils cited by Alfred Wegener as a line of evidence to corroborate his theory of continental drift (Du Toit, 1937). The epicontinental Whitehill-Irati Sea was home to all three mesosaurid species: *Brazilosaurus sanpauloensis* Shikama and Ozaki 1966, *Mesosaurus tenuidens* Gervais 1865, and *Stereosternum tumidum* Cope 1886. The majority of studies place them among Parareptilia (e.g. Modesto, 2006; Mac-

Dougall et al., 2017, 2018; Tsuji and Müller, 2009), whereas others suggest that mesosaurs may instead represent the basalmost clade of Reptilia sensu Modesto and Anderson (2004) (Laurin and Reisz, 1995; Laurin and Piñeiro, 2017).

In addition to their importance in geology, mesosaurs are also renowned for being the very first secondarily marine amniotes. Alongside the geological evidence, their aquatic lifestyle is supported by several anatomical characteristics: the elongated body, skull, neck and tail; the presence of pachyostosis in the entire skeleton of *Mesosaurus* (de Ricqlès and de Buffrénil, 2001; Modesto, 2010); and their paddle-like autopods. Furthermore, mesosaurs have been suggested to be viviparous (Piñeiro et al., 2012) and to display humeral microanatomy consistent with a marine lifestyle (Canoville and Laurin, 2010).

However, the degree to which they were aquatic is controversially discussed, and whether they might have been partially terrestrial is also still debated. Morphological evidence suggests limited in-land locomotive abilities (Modesto, 2006; Núñez Demarco et al., 2018). For some authors (Romer, 1956; Carroll, 1982; Chiappe and Chinsamy, 1996), the specialized dentition of mesosaurs was used for filter feeding, while Pretto et al. (2012) see in the tooth microstructure of *Stereosternum* evidence for an active aquatic predatorial behaviour. In their estimation of swimming speed for *Mesosaurus*, Villamil et al. (2016) came to the conclusion that this species was a slow swimmer living in shallow waters, feeding on slow prey, or possibly filter feeding, rather than actively pursuing rapid prey. To finish, Núñez Demarco et al. (2018) argued that the axial skeleton of *Mesosaurus* displays a semi-aquatic morphometric pattern, suggesting that "maybe only juveniles and young adults inhabited aquatic environments" while "more mature individuals might hypothetically have spent time on land".

Regardless of whether mesosaurs lived constantly in shallow marine environments or only during certain phases of their life, as they are the first secondary aquatic tetrapods, the course of their adaptation to living in water bears important insights into general patterns and processes triggering this specialization. For this reason, the histology of *Mesosaurus* and *Stereosternum* has been investigated by several authors (Nopcsa and Heidsieck, 1934; de Ricqlès, 1974; de Ricqlès and Buffrénil, 2001; Canoville and Laurin, 2010). They found that skeletal elements were affected by two main mechanisms resulting in a bone mass increase: (1) pachyostosis, which ensues from the hyperplasia of the periosteal cortex, generally results in the swollen appearance (hypertrophy) of bones and is particularly well expressed in the banana-shaped ribs of *Mesosaurus*; and (2) osteosclerosis, which corresponds to an increased compactness of the inner bone structure, is achieved through the condensing of the medullary regions by the retaining of calcified cartilage and/or by endosteal deposits. The retaining of calcified cartilage is the result of incomplete endochondral ossification, indicating paedomorphosis, whereas intensive endosteal de-

posits follow after complete substitution of calcified cartilage, indicating that endochondral ossification is quite complete (de Ricqlès and Buffrénil, 2001). Thus, both of these processes lead to osteosclerosis, but completely different processes are involved.

Despite having been the subject of multiple studies, histology in mesosaurs has always been examined through the prism of adaptation to living in water. Only a few specimens have been studied firsthand (Nopcsa and Heidsieck, 1934; de Ricqlès, 1974) and then referred to in other studies (de Ricqlès and Buffrénil, 2001; Canoville and Laurin, 2010). Growth and ageing patterns of their bones (skeletochronology) were virtually not investigated, except for one morphological study based on size ratio comparisons and involving only two specimens (Bickelmann and Tsuji, 2018).

Herein we perform the first skeletochronological study of mesosaur material, including 11 individuals (mostly representing *Stereosternum*) of which in part multiple bones were sampled. This includes the first histological and microanatomical data for the mesosaur *Brazilosaurus* and largely emended and expanded knowledge on *Stereosternum*, of which previously only ribs were studied.

Institutional abbreviation

– BSPG: Bayerische Staatssammlung für Paläontologie und Geologie, Munich, Germany.

– IGPB: Institut für Geowissenschaften, Paläontologie, Universität Bonn, Bonn, Germany.

– MB: Museum für Naturkunde, Leibniz-Institut für Evolutions- und Biodiversitätsforschung, Berlin, Germany.

– SMNK: Staatliches Museum für Naturkunde, Karlsruhe, Germany.

2   Material and methods

2.1   Material

Long bones, ribs, a haemal arch, and vertebrae from 10 individuals of *Stereosternum* and two ribs of 1 individual of *Brazilosaurus* were sampled for bone histological study (Table 1). Little information is available regarding the respective localities of these specimens aside from the fact that they all originate from the Irati Formation in southern Brazil. Multiple samples were taken from each individual (Table 1).

With the exception of the specimen of *Brazilosaurus* (BSPG 1965 I 131), all specimens were historically labelled as *Mesosaurus brasiliensis* but we reidentified them as *Stereosternum tumidum* based on diagnostic features such as the number of presacral vertebrae and, if available, the head/neck proportion (see Araújo, 1976; Oelofsen and Araújo, 1987; Modesto, 1999). Apart from MB.R.1988, all individuals are

fairly complete, with only individual limb elements or parts of the tail missing. MB.R.5605 is the most complete individual in our sample with an exceptionally complete tail preserved. This individual and its bone proportions served as a proxy for the reconstruction of body length estimates for less complete individuals (Table 1). MB.R.1988 is the least complete specimen and consists of one slab bearing two spatially distinct series of articulated vertebrae. One of the series (hereafter referred to as MB.R.1988a) displays 19 articulated dorsal vertebrae with ribs (12.5 cm in length) associated with a humerus. The other series (MB.R.1988b) consists of 13 posterior dorsal vertebrae (7 cm in length) and is also associated with a humerus. Both vertebral series are segments of the dorsal section of the spine and thus cannot possibly belong to the same individual. MB.R.1988a is recognized as *Stereosternum* based on the presence of 19 dorsals, which exceed the total number of dorsal vertebrae present in either *Brazilosaurus* or *Mesosaurus* (both 18), as well as based on the moderate pachyostosis of its ribs. By contrast, the identification of MB.R.1988b can only be speculative due to the absence of informative characteristics, and it is hereafter assumed that it belongs to *Stereosternum* like its neighbouring specimen.

2.2 Methods

Ribs were sampled transversally at their proximal-medial parts, where the growth record is best preserved (Klein et al., 2019). The Y-shaped haemal arch was cut transversally three times: two times proximally, where it consists of two processes, and one time at the single distal process. The plane of longitudinal vertebral sections is close to the sagittal plane in vertebrae of IGPB R 622 and matches it exactly in vertebrae of IGPB R 623. Whenever possible, long bones (humerus, femur, radius) were cut along a transverse plane at the narrowest point of the midshaft, which usually preserves the most complete growth record. However, preservation did not always allow this procedure: the humerus of BSPG 1975 I 165 was sampled distally to this point; and the femora of BSPG 1975 I 165, SMNK Pal 3806, and SMNK Pal 3808 were sectioned more proximally. All samples were processed into standard petrographic thin sections (Klein and Sander, 2007; Padian and Lamm, 2013). The thin sections were observed under a Leica DM2500LP polarizing microscope. Digital photomicrographs were taken with a Leica DFC420 mounted colour camera and edited using the 2007 Leica Image Access EasyLab 7 software. The bone histological terminology used in this study follows Francillon-Vieillot et al. (1990). The surface ratio between the medullary and cortical region (Table 2) and bone compactness were measured with a pixel-counting computer program (© Peter Göddertz, IGPB).

Body size and ontogenetic stages of specimens

In our sample the maximum body length of a *Stereosternum* individual is 69 cm (MB.R.5605; Table 1). Because humerus and femur length are available for this specimen we use MB.R.5605 as the reference specimen (100 %) for our body length calculations (Table 1). However, body proportions and ratios seem to be quite variable among mesosaurs (Table 1), and our reconstructions of body length in *Stereosternum* have to be used with care and are best regarded as a rough estimation. For instance, MB.R.2897, which is overall smaller than MB.R.5605, has longer humeri and femora than the latter. Besides, several calculated body lengths based on either humerus or femur dimensions turn out to be smaller than the actual measured body length (Table 1).

All the sampled individuals are larger than 50 cm and thus well beyond 65 % of the maximum known body length. Based on size, the state of ossification of carpal and tarsal bones, and the degree of fusion of cranial and axial elements, most of our specimens are estimated to be adults, i.e. have reached skeletal maturity. Only SMNK Pal 9165 is not fully grown based on these morphological characteristics.

3 Results

3.1 Shape of cross sections

The shape of the humeral cross sections is variable, spanning from triangular (BSPG 1975 I 165) to elliptical (IGPB R 622, MB.R.1988a) and circular (SMNK Pal 3808; MB.R.1988b) (Fig. 1; Table 2). Although some dorsoventral compaction of bones has occurred during fossilization, none of the humeri show a crushed inner bone structure. The morphology of the shaft affects the apparent histology, and in particular the readability of the growth record. If this shape is oval or circular, the growth record is regularly preserved all around the cross section; if it is somehow angled or more triangular, growth marks tend to merge where the cortex becomes thinner and to split where the cortex gets thicker.

The cross section of the radius of BSPG 1975 I 165 is egg-shaped (Fig. 2g, h). Femoral cross sections of SMNK Pal 3806 and SMNK Pal 3808 are sub-circular (Fig. 2c–f), but sampling was not carried out at midshaft. Only half of the cross section of femur IGPB R 623 (midshaft sample) is preserved (Fig. 2a, b). Its semicircular shape suggests that the complete section would have been elliptical. The shape of all rib cross sections is rather uniform, varying from a pointed oval in the proximal end to round in the median part (Figs. 3; S1 in the Supplement).

3.2 Microanatomy

All sampled long bones share the lack of an inner medullary cavity. Instead they accommodate a medullary region entirely filled with endosteal bone (Figs. 1, 2). The farther from mid-
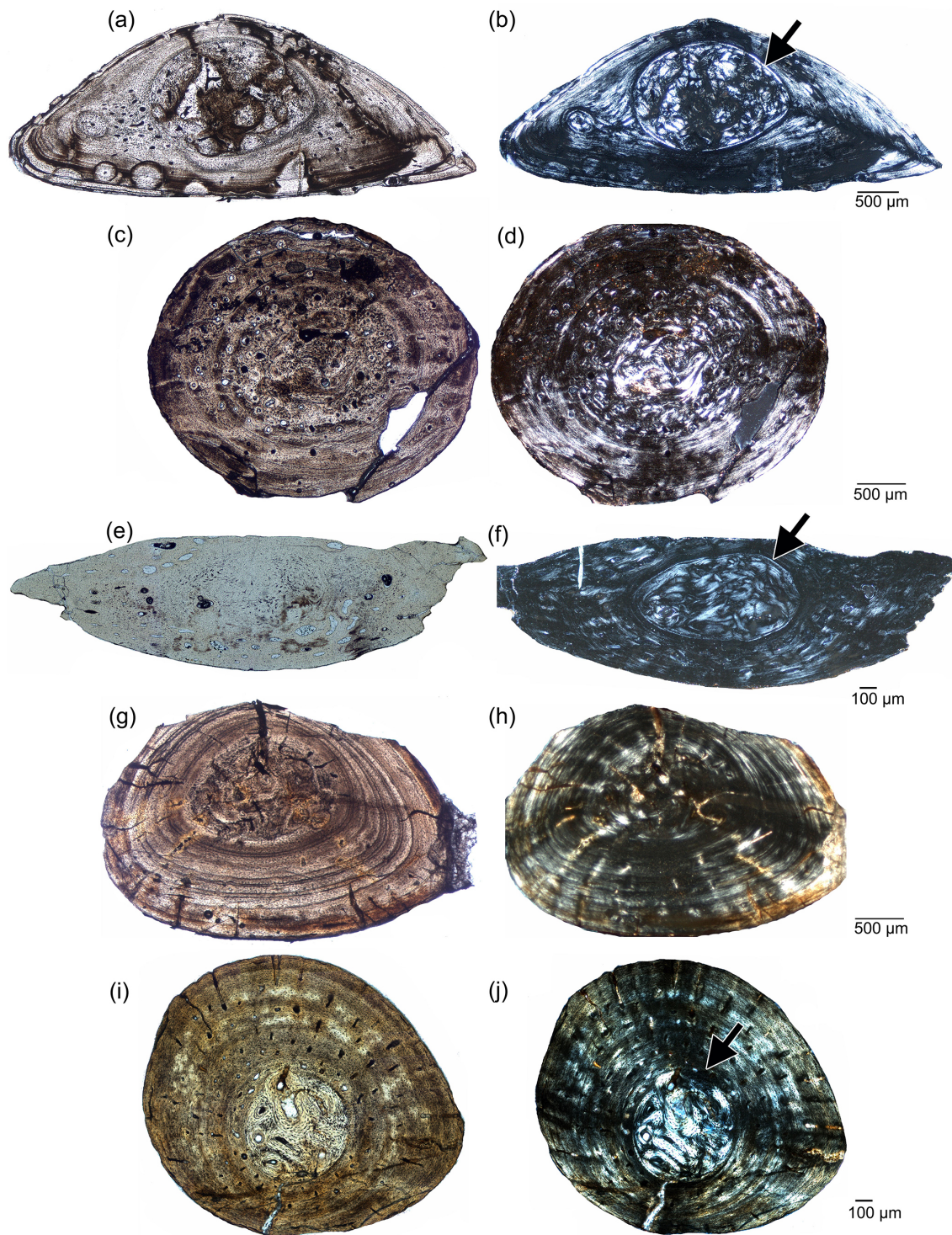
Figure 1. Composite microscopic photographs of humeral cross sections of different individuals of the mesosaur *Stereosternum* in normal **(a, c, e, g, i)** and polarized light **(b, d, f, h, j)**. **(a, b)** Humerus cross section of specimen BSPG 1975 I 165. Sample location is not exactly midshaft. **(c, d)** Humerus cross section of specimen SMNK Pal 3808. Sample location is exactly midshaft. **(e, f)** Humerus cross section of specimen IGPB R 622. Sample location is not exactly midshaft. **(g, h)** Humerus cross section of specimen MB.R.1988a. Sample location is exactly midshaft. **(i, j)** Humerus cross section of specimen MB.R.1988b. Sample location is nearly midshaft. Note the sharp line surrounding the medullary region, which separates the endosteal from the periosteal domain in humerus BSPG 1975 I 165, IGPB R 622, and MB.R.1988b (indicated by arrows).
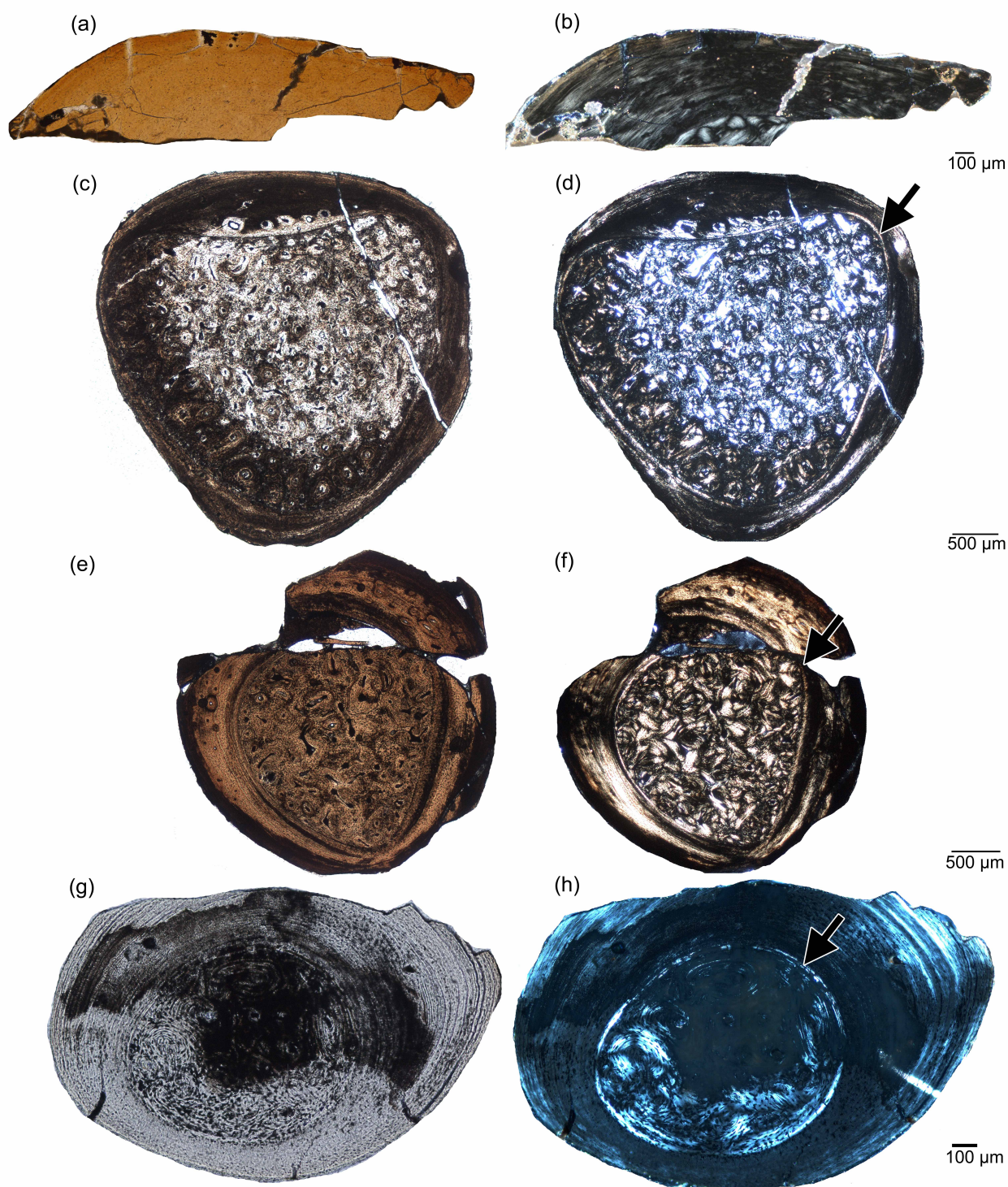
Figure 2. Composite microscopic photographs of femoral cross sections of different individuals of the mesosaur *Stereosternum* in normal **(a, c, e)** and polarized light **(b, d, f)**. **(a, b)** Femur cross section of specimen IGPB R 623. Sample location is not exactly midshaft. **(c, d)** Femur cross section of specimen SMNK Pal 3808. Sample location is distal to midshaft. Note the high amounts of calcified cartilage **(e, f)** Femur cross section of specimen SMNK Pal 3806. Sample location is distal to midshaft. Note the sharp line surrounding the medullary region, which separates the endosteal from the periosteal domain in non-midshaft samples of femur SMNK Pal 3806 and SMNK Pal 3808 as well as in radius BSPG 1975 I 165 **(g, h)** (indicated by arrows).

Table 1. Measurements of sampled specimens (in mm) of *Stereosternum* and *Brazilosaurus* (BSPG 1965 I 131). Abbreviations: fe, femur; hu, humerus; mbl, measured body length.

Specimen number/ % of max body size	Body length/ *calculated/	% of max body length (690)	Humerus length	Femur length	Sampled bones
Stereosternum					
IGPB R 623	> 650 *724 (fe)	94 % (mbl) 84 % (hu) 105 % (fe)	32	39	humerus femur dorsal rib dorsal vertebrae
BSPG 1975 I 165	> 50 cm *716 (hu and fe)	112 % (hu) 95 % (fe)	36	35	humerus radius dorsal ribs
MB R 5605	69 cm	100 %	38	37	haemal arch
SMNK Pal 3808	> 64 cm *683 (hu and fe)	103 % (hu) 95 % (fe)	39	35	femur dorsal rib
MB R 2897	64 cm	92.8 % (mbl) 86.8 % (hu) 108 % (fe)	33	40	dorsal rib
SMNK Pal 3806	> 63 cm *626 (hu and fe)	89.5 % (hu) 92 % (fe)	34	34	femur dorsal ribs
IGPB R 622	610	88 % (mbl) 83.4 % (hu) 76 % (fe)	26.7	28.1	humerus dorsal dorsal rib dorsal vertebrae
MB R 1988a	*604 (hu)	87.5 % (hu)	28	NA	humerus dorsal rib
SMNK Pal 9165	> 51 cm *571 (hu and fe)	79 % (hu) 86.5 % (fe)	30	32	dorsal ribs
MB R 1988b	*517.5 (hu)	75 % (hu)	24	NA	humerus dorsal rib
Brazilosaurus					
BSPG 1965 I 131	> 26 cm *526 (hu and fe)	68.4 % (hu) 84 % (fe)	26	31	dorsal ribs

NA: not available

shaft the sample was taken, the larger the medullary region (Table 2). Bone compactness of midshaft samples of long bones is 96 % in the well-vascularized humerus MB.R.1988a (Fig. 1i, j) and in all others 100 %.

Every proximal rib sample (except for that of IGPB R 623, which lacks any cavity; Fig. 3a, b) bears a very small sized, round medullary cavity (Fig. 3) surrounded by a moderately sized medullary region filled with endosteal bone (the free medullary cavity together with the surrounding medullary region make between 4 % and 15 % of the entire cross section, Table 2), while the enlarged medullary regions (about 25 % of cross section) of medial rib samples are completely occupied by endosteal bone (e.g. Fig. S1m, n). The proximal rib sample of *Brazilosaurus* displays a large medullary region, which occupies about 24 % of the entire cross section, whereas this region represents about 41 % of the me-

dian sample (Figs. 4, 8a). Bone compactness of rib samples of *Stereosternum* is about 97 % in the well-vascularized ribs of MB.R. 2897, SMNK Pal 3806, 98.5 % in proximal rib IGPB R 623, and 100 % in all others, including the ones of *Brazilosaurus*.

The proximal part of the haemal arch of MB.R.5605 has only a very small medullary region ($\sim$ 3 % of cross section) that contains one large erosion cavity, whereas the distal part displays a large medullary region (41 % of cross section) (Fig. 3g–j).

All sampled vertebrae, centra and neural arches alike, depict large compact endosteal territories filled with small erosion cavities but lack larger cavities (Fig. 3k, l).

In all bones, compact medullary regions are surrounded by a compact cortex, resulting in high bone compactness values and clearly indicating osteosclerosis.

Table 2. Histological features and growth record of *Stereosternum* and *Brazilosaurus* (BSPG 1965 I 131). Abbreviations: cc, calcified cartilage; eb, endosteal bone; gm, annual growth marks/rest lines; LAGs, lines of arrested growth; lb, lamellar bone; pfb, parallel-fibred bone; po/pos, primary osteon(s); sl, sharp line separating the periosteal from the endosteal domain; sec. ost, secondary osteons; svc, simple vascular canals. The percentage value in the second column refers to the surface ratio that the medullary region (i.e. usually filled by endosteal bone) occupies when compared to the cortical region.

Specimen number	Medullary region	Bone tissue	Vascularization	Periosteal erosion/ secondary osteons	Growth record
Stereosternum					
IGPB R 623					young, no distinct LAG, maybe died in its second or third year
Humerus (not mid-shaft; circular cross section)	81.37 %, no sl, high amounts of cc and eb	thin cortex highly organized pfb	avascular	none, sec. ost.	2 annuli
Femur	∼ 11.5 %, no sl, eb, no cc	inner cortex pfb, outer cortex higher organized pfb and lb	avascular	none, sec. ost.	1 indistinct rest line, supported by a change in tissue organization
Proximal rib sample	11.67 %, sl, some remains of cc between eb	pfb and lb	well-vascularized inner and middle cortex, svc and pos	scattered, moderate amount of sec. ost.	4 changes in tissue but no distinct rest line
Median rib sample	16.2 %, sl, some cc between eb	pfb and lb	well-vascularized inner and middle cortex, svc and pos	scattered, moderate amount of sec. ost.	1 change in tissue and 1 indistinct rest line
BSPG 1975 I 165					died in its fourth to fifth year of life
Humerus (triangular cross section; not exactly sampled at midshaft)	24.3 %, sl, no cc	inner cortex pfb, outer cortex higher organized pfb and lb	moderate vascularization; svc and pos at the inner cortex of one bone side, more scattered at the postaxial side	few scattered sec. ost.	3 major gm (LAGs accompanied by multiple rest lines) and one change in bone tissue in the inner cortex
Radius	28.6 %, sl, no cc	highly organized pfb/lb	avascular	none, sec. ost.	multiple rest lines, 4 major cycles are identified and one change in bone tissue in the inner cortex
Proximal rib (oval)	6.7 %, sl, no cc	highly organized pfb/lb	avascular	few scattered sec. ost.	multiple rest lines, 4 major cycles are identified and one change in bone tissue in the inner cortex
Proximal rib (round)	6.5 %, sl, no cc	highly organized pfb/lb	avascular	few scattered sec. ost.	multiple rest lines, 4 major cycles are identified and one change in bone tissue in the inner cortex
MB R 5605					died in its fourth to fifth year of life
Haemal arch					4 double LAGs
Proximal	3 %, sl, some cc	pfb	avascular	none, sec. ost.	2 indistinct gm
Distal	40.6 %, sl, no cc	highly organized pfb/lb	avascular	few erosion cavities sec. ost.	3–4 gm

Table 2. Continued.

Specimen number	Medullary region	Bone tissue	Vascularization	Periosteal erosion/ secondary osteons	Growth record
SMNK Pal 3808					died in its fifth year of life
Humerus (midshaft; circular cross section)	7.2 %, no sl, few remains of cc	pfb	low vascularization; few scattered svc and pos	few scattered sec. ost.	3 gm multiple rest lines
Femur (not midshaft)	68.34 %, sl, high amount of cc	highly organized pfb	avascular	few scattered sec. ost.	1 gm
Proximal rib sample	6.7 %, sl, no cc	highly organized pfb/lb	low vascularization; few scattered svc and pos	few scattered sec. ost.	3 major cycles, each consisting of multiple rest lines; third one consists of three widely spaced rest lines in all four samples
MB R 2897					died in its fourth year of life
Proximal rib	15 %, sl, no cc	highly organized pfb/lb	moderately vascularized svc and few pos	few erosion cavities; scattered sec. ost.	3 LAGs accompanied by tissue changes
SMNK Pal 3806					died in its sixth year of life
Femur (not midshaft)	43 %, sl, few remains of cc	highly organized pfb/lb	low vascularization svc and few pos	few scattered sec. ost.	4 growth mark (multiple rest lines)
Proximal rib sample	9.15 %, sl, no cc	vascularized part loose organized pfb, avascular part highly organized pfb/lb	moderate vascularization (svc and pos) in one direction, avascular at the other side	scattered sec. ost. in one direction	5 growth marks (multiple rest lines)
Median rib sample	11.74 %, sl, high amounts of cc	vascularized part loose organized pfb, avascular part highly organized pfb/lb	moderate vascularization (svc and pos)	scattered sec. ost.	5 growth marks (multiple rest lines)
IGPB R 622					died in its first year of life
Humerus (midshaft but slightly compressed; elliptical cross section)	20.18 %, sl, locally restricted remains of cc	cc, pfb	avascular	some very large erosion cavities	0 gm
Proximal rib	4.1 %, sl, no cc	pfb	avascular	few erosion cavities grading into sec. ost.	0 gm
Median rib	25 %, sl, high amounts of cc	pfb	avascular	few erosion cavities grading into sec. ost.	
MB R 1988a					died in its seventh year of life
Humerus (midshaft; elliptical cross section)	no sl, 14.4 % med. reg., filled by eb, no cc	highly organized pfb/lb	avascular	few scattered erosion cavities	6 major gm (double–multiple rest lines)
Proximal rib	6.2 %, no sl, no cc	highly organized pfb/lb	avascular	none	6 major gms (multiple rest lines)
SMNK Pal 9165					died in its fourth year of life
Proximal rib	6.96 %, sl, no cc	highly organized pfb/lb	avascular	none	3 LAGs (double ones) plus 1 tissue change in the inner cortex
Proximal rib	4.84 %, sl, no cc	highly organized pfb/lb	avascular	none	3 LAGs (double ones) plus 1 tissue change in the inner cortex

Table 2. Continued.

Specimen number	Medullary region	Bone tissue	Vascularization	Periosteal erosion/ secondary osteons	Growth record
MB R 1988b					died in its first or second year of life (or is maybe even younger)
Humerus (midshaft; circular cross section)	12.6 %, sl, no cc	pfb	moderately vascularized radial and longitudinal svc	none	4 changes in colour/ tissue, 1–2 indistinct rest lines
Proximal rib	12 %, sl, no cc	pfb	avascular	none	4 changes in color/ tissue, 1–2 indistinct rest lines
Brazilosaurus					
BSPG 1965 I 131					died in its seventh year of life
Proximal rib	24 %, sl, no cc	highly organized pfb/lb	avascular	none	6 major gms; multiple, closely spaced rest lines
Proxi-median rib	26 %, sl, locally remains of cc	lb	avascular	few scattered sec. ost.	multiple, closely spaced rest lines
Median rib	41 %, sl, locally remains of cc	lb	avascular	none	multiple, closely spaced rest lines

3.3 Histological description

3.3.1 Medullary regions and occurrence of calcified cartilage in the endosteal domain

When sampling has not been carried out exactly at mid-shaft in long bones, the endosteal and periosteal domains are demarcated by a sharp line (see Klein and Griebeler, 2018) (Table 2). Except for femur IGPB R 623, humeri SMNK Pal 3808 and MB.R.1988a, and the proximal rib sample of MB.R.1988a, all samples show such a sharp line (Table 2), meaning that the best sampling location is very restricted. The medullary regions of *Stereosternum* samples consist of endosteal bone and only a few samples show calcified cartilage (Table 2). Calcified cartilage occurs in the endosteal domains of the vertebral centra (Fig. 3k, l) and along their notochordal canal through the centrum. In ribs and long bones, high amounts of calcified cartilage are found only in non-midshaft humerus and femur samples (IGPB R 623, Fig. 5f; SMNK Pal 3808), in the proximo-medial rib of IGPB R 622, and in one median rib sample of SMNK Pal 3806. Moderate remains of calcified cartilage occur in the proximal and median rib of IGPB R 623, whereas the femur of the same individual shows no calcified cartilage at midshaft. Calcified cartilage occurs locally restricted in the humeri of IGPB R 622 (Fig. 5e) and SMNK Pal 3808 (Fig. 5a), in the non-midshaft femur sample SMNK Pal 3806 (Fig. 5g), and in the distal sample of the haemal arch (MB.R.5606, Fig. 3i, j). Bones of individuals BSPG 1975 I 165 (Fig. 5b), MB.R.1988a (Fig. 5c), and

MB.R.1988b (Fig. 5d) as well as the rib samples MB.R.2897 and SMNK Pal 9165 do not show any calcified cartilage. Thus, there is no clear pattern (i.e. sampling location) associated with the presence of calcified cartilage in our sample of *Stereosternum*.

The proximal sample of the *Brazilosaurus* rib does not show any calcified cartilage, but the medial one bears some locally restricted clusters in its medullary region (Fig. 4f).

3.3.2 Bone tissue and vascularization in the periosteal domain

In all *Stereosternum* samples, bone is mainly formed by parallel-fibred tissue. It occurs in different degrees of organization, from loosely to highly organized (Fig. 6), sometimes partially turning into lamellar tissue (Fig. 6b). Osteocyte lacunae are large and numerous but often flattened. In long bones and ribs, vascularization is dominated by simple longitudinally oriented vascular canals, which are sometimes fully or partially lined with lamellar bone, resulting in complete or incompletely primary osteons (Klein, 2010; Table 2). Primary osteons are often secondarily widened (Figs. 6d, 8b). In some samples, vascular canals and primary osteons are intermixed with erosion cavities and/or young (i.e. wide open; Currey, 2002) secondary osteons (Table 2; Fig. 6d). The humerus of IGPB R 622 bears very large, irregularly shaped, erosion cavities along its dorso-preaxial and ventro-postaxial edges (Fig. 6e). The humerus of MB.R.1988b shows the highest vascular density. Its cortex consists of mainly longitudinally and some radially arranged simple canals (Fig. 6g).
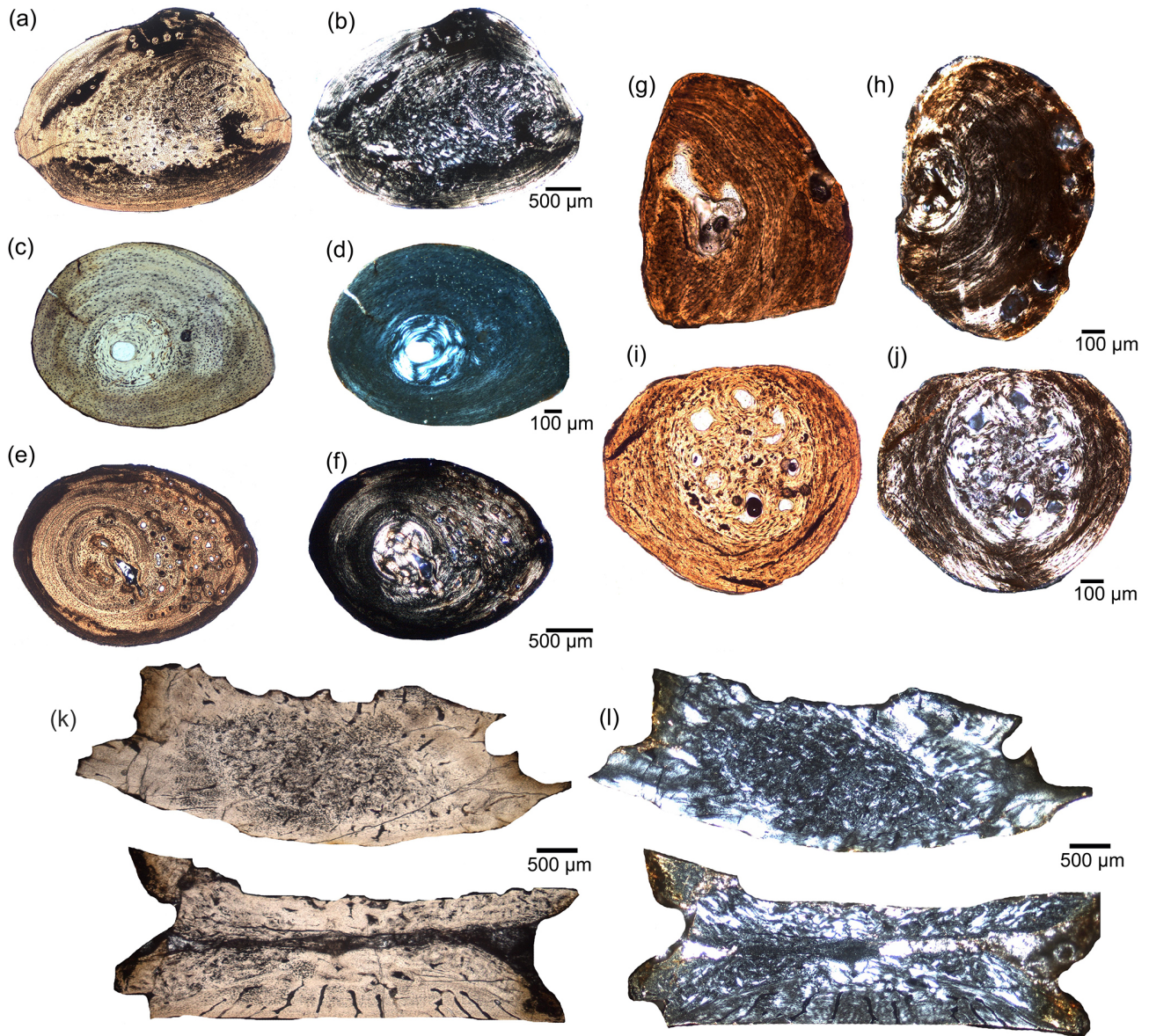
Figure 3. Microscopic photographs of cross sections of rib samples of different individuals of the mesosaur *Stereosternum*. The variability of shapes of rib cross sections is due to different sampling location along the proximal to the median part of the rib shaft as well as due to different anatomical position along the trunk region (see also Fig. S1). Proximal to median rib sample of IGPB R 623 in normal **(a)** and polarized light **(b)**. Proximal rib sample of MB.R.1988b in normal **(c)** and polarized light **(d)**. Proximal to median rib sample of SMNK Pal 3806 in normal **(e)** and polarized light **(f)**. Proximal part of haemal arch of MB.R.5606 in normal **(g)** and polarized light **(h)**. Distal part of haemal arch of MB.R.5606 in normal **(i)** and polarized light **(j)**. Dorsal vertebra in normal **(k)** and polarized light **(l)**.

However, most samples are lightly vascularized or even avascular (Fig. 6a, b, f, h; Table 2). Vascular density in the ribs is well correlated with that in the long bones in individual MB.R.1988a and IGPB R 622 (both avascular), SMNK Pal 3808 (low vascular density), and SMNK Pal 3806 (moderate vascular density) (Figs. 1, 3; S1). There is no such correlation in BSPG 1975 I 165 and MB.R.1988b, which both have a well-vascularized humerus but lightly vascularized or even avascular ribs, or in IGPB R 623, in which on the

contrary the femur is avascular but the ribs are well vascularized. The haemal arch of *Stereosternum* is avascular (Fig. 3g–j). Scattered erosion cavities and/or secondary osteons are the only form of periosteal remodelling, and it does not affect the completeness of the growth record. Periosteal (dorsal and ventral part) and endochondral (anterior and posterior part) territories of vertebrae (sensu de Buffrénil et al., 2008) are distinguishable, but not as clearly as in eosauropterygians (Klein et al., 2019). The endosteal bone is more compact than
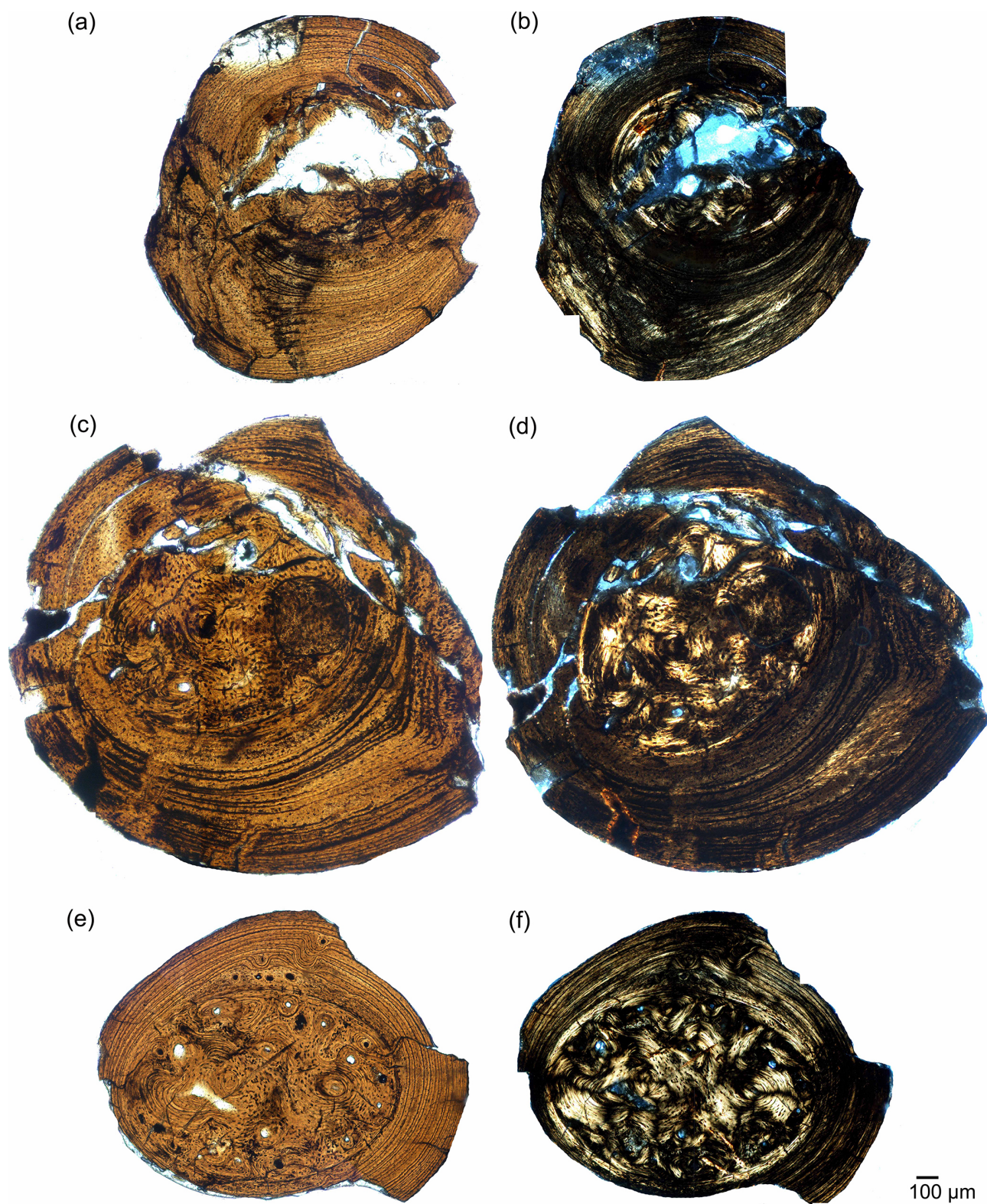
Figure 4. Composite microscopic photographs of rib samples of *Brazilosaurus* (BSPG 1965 I 131). Proximal part of dorsal rib in normal (**a**) and polarized light (**b**). Proximal to median part of dorsal rib in normal (**c**) and polarized light (**d**). Median part of dorsal rib in normal (**e**) and polarized light (**f**).
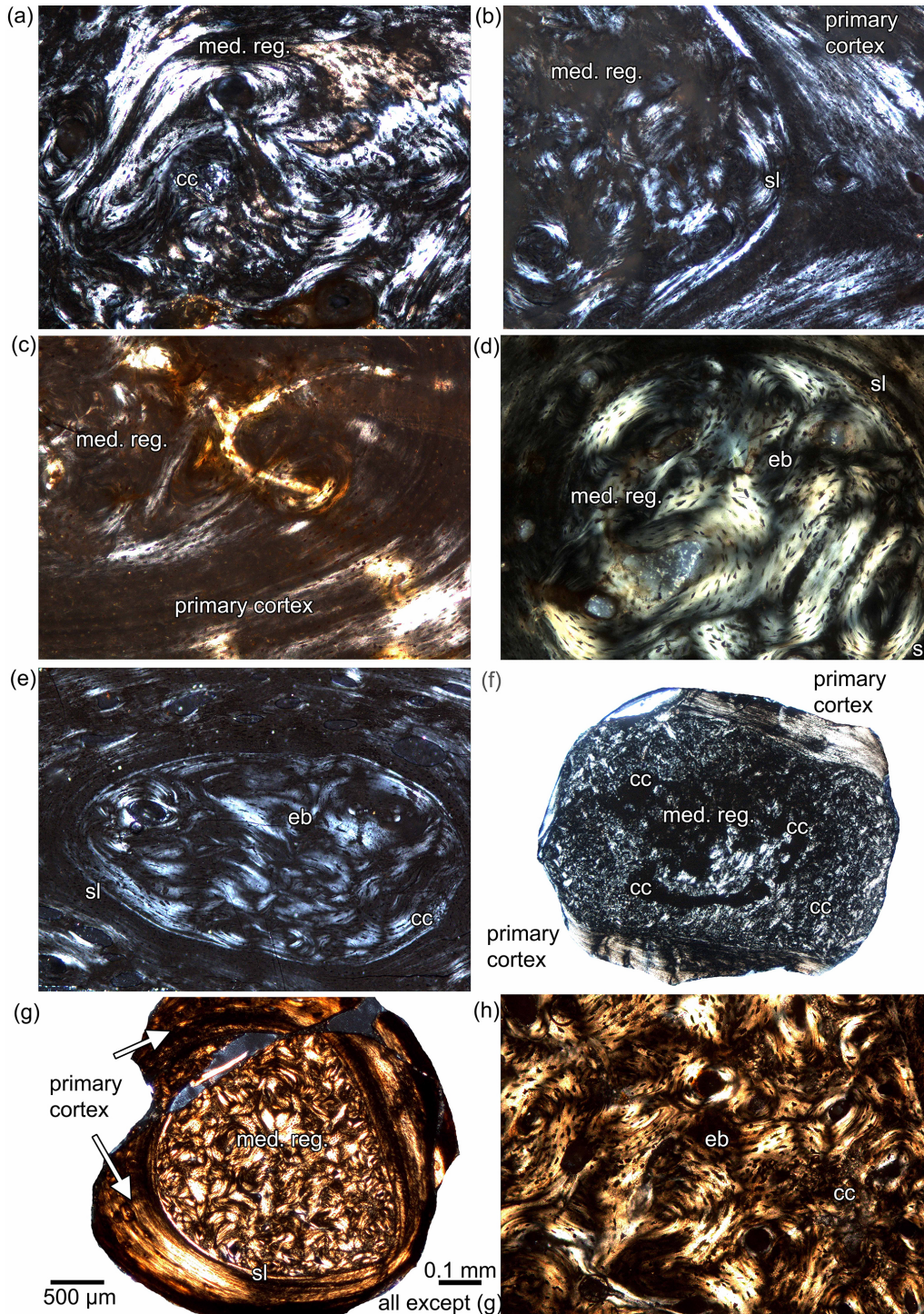
Figure 5. Details of medullary regions in long bones of *Stereosternum* in polarized light. **(a)** Medullary region depicting clusters of calcified cartilage between the endosteal bone in midshaft sample of humerus SMNK Pal 3808. **(b)** Medullary region depicting endosteal bone and a sharp line (sl) but no calcified cartilage in humerus BSPG 1975 I 165. **(c)** Medullary region depicting endosteal bone but no calcified cartilage and sharp line in midshaft sample of humerus MB.R.1988a. **(d)** Medullary region consisting of endosteal bone in midshaft sample of humerus MB.R.1988b. **(e)** Medullary region consisting of endosteal bone with clusters of calcified cartilage at the margin of the sharp line in non-midshaft sample of humerus IGPB R 622. **(f)** Enlarged medullary region consisting largely of calcified cartilage and the reduced cortex in non-midshaft sample of humerus IGPB R 623. **(g)** Non-midshaft sample of femur SMNK Pal 3806. The medullary region is enlarged but consists mainly of endosteal bone, only clusters of calcified cartilage occur. **(h)** Detail of **(g)**. Abbreviations: cc, calcified cartilage; eb, endosteal bone; sl, sharp line.
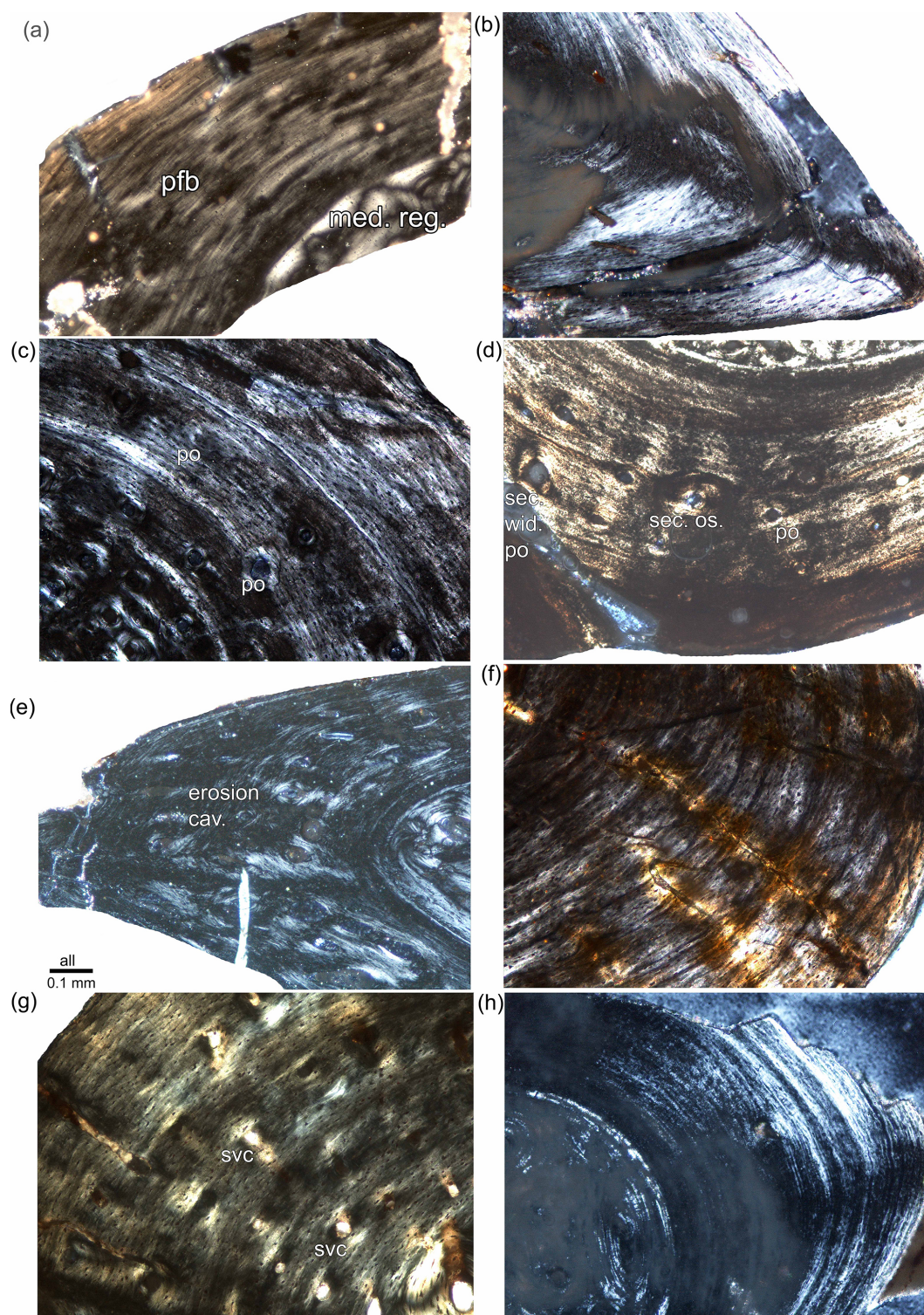
Figure 6. Details of *Stereosternum* long bone tissue all in polarized light/under crossed nicols. All showing parallel-fibred bone tissue in different degrees of organization. **(a)** Avascular, highly organized parallel-fibred tissue in femur IGPB R 623. **(b)** Avascular, highly organized parallel-fibred tissue partially grading into lamellar tissue in humerus BSPG 1975 I 165. **(c)** Some vascularization by incipient primary osteons in a matrix of parallel-fibred tissue in the inner cortex of humerus SMNK Pal 3808. **(d)** Simple vascular canals and incipient primary osteons in a matrix of parallel-fibred tissue in the outer cortex of femur SMNK Pal 3806. **(e)** Simple vascular canals and lightly organized parallel-fibred tissue in humerus IGPB R 622. **(f)** Highly organized avascular parallel-fibred tissue partially grading into lamellar tissue in humerus MB.R.1988a. **(g)** Lightly organized parallel-fibred tissue with simple vascular canals in humerus MB.R.1988b. **(h)** Highly organized parallel-fibred tissue partially grading into lamellar tissue in radius BSPG 1975 I 165.

the periosteal bone (Fig. 3k, l). The layer of compact periosteal cortex is thicker in the ventral part of the centrum than in the dorsal one. The ventral part of the centrum is traversed by large, simple, radially running vascular canals, whereas those innervating the neural arch are rarer, smaller, more irregularly shaped and randomly scattered. The dorsal vertebrae clearly show a notochordal canal through the centrum, occupied by cartilage cells.

The rib samples of *Brazilosaurus* display avascular lamellar bone (Table 2; Fig. 4).

3.4 Growth record

Neither growth marks nor any evidence of cyclical growth is visible in the vertebrae. Because of the lack of intensive periosteal remodelling in midshaft samples of long bones and proximal samples of ribs, the growth record is complete in these bones; i.e. no inner growth marks seem to be lost due to remodelling. In most specimens of *Stereosternum* and in the ribs of *Brazilosaurus*, annual growth cycles are represented by distinct lines of arrested growth (LAGs). These are often accompanied by additional rest lines (Fig. 7), resulting in the presence of double or multiple lines at the end of each annual growth cycles, making an exact count difficult. Furthermore, a single LAG can split and further merge back with itself again (Fig. 7). This, along with the absence of changes in tissue organization or vascularity, hampers annual growth mark count. The growth mark count for each sample is given in Table 2. In general, the number of growth marks seems to correspond in long bones and ribs of the same individual (Table 2).

Yet, in two humeri of *Stereosternum* individuals (IGPB R 623, Fig. 1e, f; MB.R.1988b, Fig. 1i, j) and one rib sample (IGPB R 623, Figs. 3a, b, S1m, n), growth marks are not represented by distinct LAGs. Instead, the cortex is stratified by accumulations of osteocyte lacunae to thin layers and/or by a change in bone tissue organization. Because all other samples of *Stereosternum* show distinct LAGs, these less pronounced growth marks, mainly those in MB.R.1988b, are not counted as annual growth marks but interpreted as subcycles stratifying the first year of life.

In bones of individual BSPG 1975 I 165 (Figs. 1c, d, 2g, h, S1a, b) and in the ribs of SMNK Pal 9165 (Fig. S1i, j), the innermost cortex also contains a large inner first cycle, which contains a change in tissue that is then followed by clear LAGs accompanied by multiple rest lines. This inner change in tissue is also not counted as an annual growth mark but interpreted as a sub-cycle, dividing the fast and large growth period in the first year of life. This large inner first cycles indicate that most (up to 50 %) of the appositional growth happened in the first year of life in *Stereosternum*.

Individual SMNK Pal 3808 shows three major growth cycles, each consisting of multiple rest lines (Fig. 1c, d). The third of these consists in the humerus and in the rib sample (Fig. S1g, h) of three widely spaced rest lines.

Neither an increase in tissue organization, a decrease in vascular density, nor a change in the spacing of rest lines is identified in any sample, and thus nothing can be said about onset of sexual maturity. Because in most samples any annual cycle ends in multiple rest lines, resembling a kind of external fundamental system, addressing the attainment of full growth is also not possible with certainty in our sample. However, only bones of individual SMNK Pal 3806 show multiple rest lines in their outer cortex, meaning that it died at the end of a growth cycle, whereas all others died sometime during the growth cycle.

The rib samples of *Brazilosaurus* depict a high number of closely spaced rest lines throughout the entire cortex, making it difficult to identify annual cycles.

4 Discussion

4.1 Comparison of mesosaur histology and microanatomy

4.1.1 General comparison

Bone tissue in *Stereosternum* and *Brazilosaurus* is lamellar-zonal, with a low (in some rare cases, moderate) degree of vascularization or being avascular. This highly organized and lightly vascularized type of bone tissue is for example characteristic of modern reptiles, of *Claudiosaurus* (de Buffrénil and Mazin, 1989) and small choristoderes (Skutschas and Vitenko, 2017). However, sauropterygians from the Triassic present less organized and more vascularized bony tissues, suggesting higher growth rates than mesosaurs (Klein, 2010; Hugi et al., 2011; Klein and Griebeler, 2018). The high degree of bone compactness in sampled long bones of *Stereosternum* is unique among marine reptiles. It exceeds that of the Permian *Claudiosaurus* (de Buffrénil and Mazin, 1989), of most Triassic marine reptiles (Klein et al., 2015a, 2016; Klein and Griebeler, 2018), and of the modern marine iguana *Amblyrhynchus* (Hugi and Sánchez-Villagra, 2012). Only pachypleurosaurs from the Alpine Triassic have comparable bone compactness values, although these are on average somewhat lower than that of *Stereosternum* (Hugi et al., 2011).

The large number of osteocyte lacunae in vertebrae samples of *Stereosternum* following the direction of bone growth in the endochondral bone is not observed in marine reptiles (Klein et al., 2019; Tanja Wintrich, personal observation) and is thus very distinctive, too.

4.1.2 Comparison of the microanatomy of mesosaur ribs

Although sample size is restricted for *Brazilosaurus* and *Mesosaurus*, and as we did not study the ribs of *Mesosaurus* firsthand, we want to mention here some preliminary observations, resulting from comparing ribs of mesosaurs. Infor-

Figure 7. Growth mark count in humerus MB.R.1988a. Note the presence of multiple rest lines at the end of cycles as well as the split and merging of some rest lines.

mation about the ribs of *Mesosaurus* is drawn from Nopcsa and Heidsieck (1934) and de Ricqlès (1974). *Mesosaurus*, *Stereosternum*, and *Brazilosaurus* share highly osteosclerotic ribs as a result of condensation of the periosteal cortex and the medullary region, with both domains lacking any spongiosa. However, as the current study documents, the surface ratio of periosteal cortex over medullary region is broader in *Stereosternum* ($\geq$ 85 %–95 % in proximal rib samples/75 % in median rib samples) than in *Brazilosaurus* ($\geq$ 75 % in proximal rib samples/60 % in median rib samples) (Table 2; Fig. 8). According to Nopcsa and Heidsieck (1934, p. 442) as well as to de Ricqlès (1974, fig. 11), the medullary region in the ribs of *Mesosaurus* is nearly as broad as the periosteal cortex (Fig. 8c–e; $\sim$ 64 % measured from de Ricqlès, 1974, fig. 11). It is unclear whether these ribs of *Mesosaurus* were sampled proximally or medially, but in terms of the ratio between the endosteal and periosteal domain, the ribs of *Mesosaurus* clearly differ from those of *Stereosternum* and are in this regard rather similar to those of *Brazilosaurus* (Fig. 8).

Brazilosaurus is characterized by a highly organized avascular lamellar tissue, regularly stratified by very clear rest lines. This tissue type is easily distinguished from that of *Mesosaurus* and *Stereosternum* (Figs. 3, 4, 8). This characteristic stratification in *Brazilosaurus* seems to be independent of ontogenetic age. As for them, *Mesosaurus* and *Stereosternum* share comparable tissue types in ribs. They both present a less organized tissue and some vascularization in the form of longitudinally simple vascular canals and primary osteons. Comparatively to *Brazilosaurus*, they are less regularly stratified by rest lines.

Thus, considering the relative size of periosteal and endosteal domains as well as the tissue type, and provided sampling was carried out in similar locations, the ribs of each taxon are very characteristic of and distinct from each other.

4.2 Pachyostosis and osteosclerosis in mesosaurs

Nopcsa and Heidsieck (1934) already pointed out that *Stereosternum* ribs are less pachyostotic and osteosclerotic than *Mesosaurus*. In terms of pachyostosis in the ribs, our specimens confirm that this genus stands somewhat in between the two other mesosaur genera, with its ribs being less pachyostotic than those of *Mesosaurus* but more so than
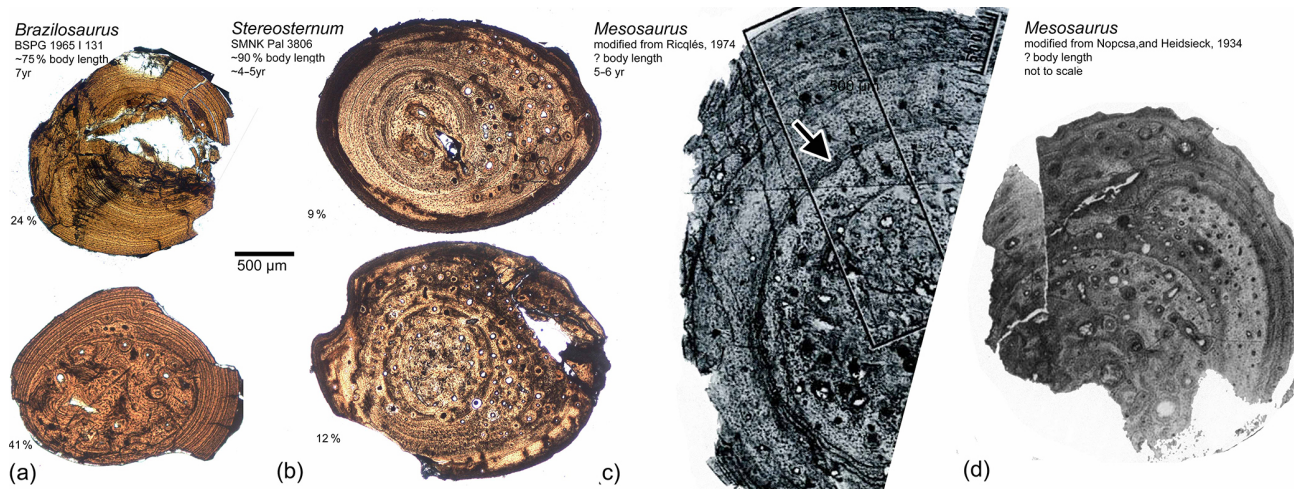
Figure 8. Comparison of mesosaur ribs. **(a)** *Brazilosaurus* (BSPG 1965 I 131) rib samples. **(b)** *Stereosternum* (SMNK Pal 3806) rib samples. **(c)** *Mesosaurus* rib sample and outline sketch modified from de Ricqlès (1974). **(d)** *Mesosaurus* rib sample modified from Nopcsa and Heidsieck (1934).

those of *Brazilosaurus*. We show that, albeit gracile, the ribs of *Brazilosaurus* are also osteosclerotic. Thus, contrary to pachyostosis *sensu stricto* (Houssaye, 2009), osteosclerosis affects the ribs of all three species to similar degrees. We further document osteosclerosis for the first time in the long bones of *Stereosternum*. The presence of osteosclerosis in all our sampled bones without pronounced pachyostosis allows us to conclude that osteosclerosis occurs early on in ontogeny.

As mentioned above, Nopcsa and Heidsieck (1934) had described pachyostosis and osteosclerosis in the ribs of *Stereosternum* and *Mesosaurus*. They mentioned an increase in the periosteal cortex and a highly condensed medullary region for both taxa. According to these authors, the medullary region was condensed by endosteal deposits in the ribs of *Mesosaurus*. In their *Stereosternum* sample, however, the centre of the rib contained high amounts of calcified cartilage. Because the ribs were also small in size, they argued that their *Stereosternum* specimen was likely a young individual. They were convinced that the microanatomy in older ontogenetic stages of *Stereosternum* would look like that in their sample of *Mesosaurus* (Nopcsa and Heidsieck, 1934, p. 444). This is confirmed by our study, where individuals larger than 65 % of the average adult length do not show high amounts of calcified cartilage. Besides, in our *Stereosternum* sample the presence or absence of calcified cartilage is not related to sampling location or specimen age (Table 2). Some individuals retain it, whereas others do not. Our results confirm the observations of Nopcsa and Heidsieck (1934) that endosteal deposits in the medullary region of ribs are the main driver of osteosclerosis, as is the case in all other bones of *Stereosternum*.

Contrary to Nopcsa and Heidsieck (1934), de Ricqlès (1974) and de Ricqlès and de Buffrénil (2001) suggested that

osteosclerosis in the ribs of *Mesosaurus* might have been caused by an incomplete endochondral ossification and the retaining of calcified cartilage. Our results do not support this hypothesis, but it is possible that the observations of de Ricqlès (1974) were nonetheless accurate if the specimen of *Mesosaurus* he studied was at an early ontogenetic stage, or if the presence of calcified cartilage in bones of *Mesosaurus* is as variable as in *Stereosternum*.

The absence of high amounts of calcified cartilage in *Stereosternum* and *Brazilosaurus* is comparable to what is known for other aquatic or semi-aquatic reptiles. In the Permian diapsid *Claudiosaurus*, osteosclerosis is also the result of intensive endosteal deposits and Haversian reconstruction (de Buffrénil and Mazin, 1989), whereas endochondral ossification is quite complete (de Ricqlès and de Buffrénil, 2001). In the case of small Early Cretaceous choristoderes, Skutschas and Vitenko (2017) showed that osteosclerosis was achieved through endosteal deposits as well, but because the humerus they studied was likely not sampled at midshaft, this result in choristoderes might not be comparable to ours on mesosaurs. Triassic pachypleurosaurs, contrary to the three previously mentioned clades, retain high amounts of calcified cartilage at the midshaft of long bones and in their ribs (Klein et al., 2019). All the aforementioned taxa are of comparably small size and are interpreted as having inhabited shallow marine or lacustrine environments. Despite this relative homogeneity in their life conditions, osteosclerosis in these clades is achieved in different ways. Thus, there does not seem to be any correlation between environmental or size-related factors and modes of osteosclerosis. Whether these processes are influenced by phylogeny or correlate with other factors must be clarified in future studies.

According to the few phylogenetic studies regarding the intra-relationships of Mesosauridae, *Brazilosaurus* repre-

sents the basalmost taxon of the clade (Rossmann and Maisch, 1999; Karl et al., 2007). While this taxon is also the least pachyostotic, it nevertheless displays an advanced degree of osteosclerosis. Thus, pachyostosis and osteosclerosis did not occur simultaneously in the evolutionary history of the clade but rather as two distinct steps. The fact that osteosclerosis occurred first suggests that increasing inner bone compactness was more crucial and possibly easier to achieve than increasing bone volume early on in the adaptation to an aquatic lifestyle. In this regard, *Brazilosaurus* is less adapted to an aquatic environment, and thus less derived, than *Stereosternum* and *Mesosaurus*.

4.3 Life history traits

Thanks to the lack of periosteal remodelling, the growth record in *Stereosternum* specimens is complete. The first growth cycle is always the largest, whereas most of the other cycles are closer and relatively evenly spaced. Considering that, based on the length of its humerus, the newborn *Stereosternum* described by Bickelmann and Tsuji (2018) would have had a body length of about 13–14 cm; and that some of our adult individuals measure between 60 and 70 cm (Table 2); and given the disparity in growth cycle width in their bones, it is safe to assume that *Stereosternum* would have experienced an enormous increase in size during its first years of life. This is comparable to juveniles of extant lepidosaurs, who can double their size in their first year (Andrews, 1982; Lin and Rieppel, 1998), or with *Alligator mississippiensis*, whose apposition rates peak during its first year of growth as well (Woodward et al., 2014). However, some specimens of *Stereosternum* reached a body length of more than 60 cm in their first or second year of life (Table 2) – an extreme leap in body size in a short time, especially considering the highly organized and lightly vascularized tissue – whereas other individuals needed up to 4 or more years to reach the same size.

As a result of this observation, *Stereosternum* shows a poor correlation between growth mark count (i.e. age) and body length (Tables 1, 2). One of the largest individuals (IGPB R 623, 94 % of the maximum body size) in the sample exhibits only two annuli that are not very distinct (Figs. 2a, b; 6a). Another relatively large individual (IGPB R 622, 88 % of the maximum body size) does not show any growth marks (Figs. 1e, f; 6e), whereas an individual at 87.5 % of the maximum body size (MB.R.1988a; Figs. 1g, h; 6f; 7) has six major growth cycles. Ribs of SMNK 9165 already show three growth marks, but on the basis of morphology it is not yet fully grown. This poor correlation between age and size might be related to several factors such as high intraspecific variation, developmental plasticity, or sexual dimorphism. However, biogeographic and/or time-related differences might be also an explanation for this discrepancy because as a result of time-averaging our specimens were likely not members of the same populations. They originated

from different localities in the widespread Irati Formation, and stratigraphic as well as environmental and climate differences cannot be excluded. It is also possible that growth marks reflect a non-yearly seasonality that would vary much more drastically depending on the environment, hence biasing the age estimate.

No indication of onset of sexual maturity was detected in the here-studied mesosaur individuals, which in other tetrapods is often indicated by a change in tissue and/or vascular organization (i.e. change in growth rate) or by a different spacing pattern of LAGs (i.e. cycle distance) (e.g. Klein and Griebeler, 2018).

Whether any of our individuals had achieved maximum size and thus stopped growing could also not be determined. The outer cortex of most samples shows avascular, highly organized parallel-fibred bone or lamellar bone. Annual growth cycles always end with multiple rest lines, which is thus not a good criterion for full growth in the current sample.

The presence of multiple rest lines at the end of each cycle indicates strong influence of exogenous and endogenous factors. It thus could represent two or several growth seasons (Castanet et al., 1993) or two or more reproduction cycles per year. The occurrence of multiple rest lines in this extent has previously been described, for example, for Triassic temnospondyls (Konietzko-Meier and Klein, 2013) and sauropterygian placodonts (Klein et al., 2015b). It is also described for modern newts (Francillon-Vieillot et al., 1990) and sea turtles (Snover and Hohn, 2004).

Based on growth mark count, the oldest of the studied *Stereosternum* individuals died in its seventh year.

The growth mark count on the ribs of the *Brazilosaurus* specimen indicates it had reached a similar age.

5 Conclusions

All bones of *Stereosternum* show strong osteosclerosis, and so do, somewhat unexpectedly, the gracile ribs of *Brazilosaurus*. In *Stereosternum* and, as far as we can evaluate on the basis of a two-rib sample, in *Brazilosaurus*, osteosclerosis is reached by intensive endosteal deposits, usually coupled with fairly complete erosion of calcified cartilage, and the inhibition of periosteal remodelling. Comparison of our results of rib histology and microanatomy with similar published data on *Mesosaurus* (Nopcsa and Heidsieck, 1934; de Ricqlès, 1974) reveals that the ribs of *Mesosaurus*, *Stereosternum*, and *Brazilosaurus* can be well distinguished histologically.

Our results further confirm an aquatic adaptation (i.e. strong osteosclerosis) for individuals of *Stereosternum* and *Brazilosaurus* over 65 % body length, favouring an aquatic lifestyle. Canoville and Laurin (2010) suggested an aquatic lifestyle for *Mesosaurus* as well, whereas Núñez Demarco et al. (2018) concluded an aquatic lifestyle only for juveniles and young adults of *Mesosaurus* but postulated a

terrestrial lifestyle for more mature individuals based on vertebrae morphology and morphometric data. In any case, the lifestyle of *Stereosternum* might have differed from that of *Mesosaurus*, because *Mesosaurus* is the only mesosaur that has pachyosteosclerotic bones.

The study of the growth record of *Stereosternum* reveals a poor correlation of body size and age in years. Some individuals of *Stereosternum* achieved most of their body size within their first or second year of life, whereas others needed several years. These observations may point to strong developmental plasticity. Life history traits such as the onset of sexual maturity or attainment of full size are not identifiable in the growth record. The maximal growth mark count in our sample is 6, suggesting that these individuals died in their seventh year of life.

Striking is the presence of double or even multiple rest lines at the end of each cycle, making exact growth mark counts difficult and pointing to a high influence of exogenous (e.g. several growth season per annum) and endogenous (e.g. several reproduction cycles per annum) factors.

In conclusion, our results provide novel insights and reveal differences in the process of aquatic adaptation in mesosaur taxa. Individuals of *Stereosternum*, having reached more than half of the maximum known body length, do not yet show pachyostosis of their ribs or other bones but already display distinct osteosclerosis. It is very interesting to note that osteosclerosis also occurs in *Brazilosaurus*, the most basal member of Mesosauridae, lacking proper pachyostosis and thus being less adapted to an aquatic environment when compared to *Stereosternum* and *Mesosaurus*.

Data availability. All thin sections are stored under the respective specimen number in the respective public collection as listed in Table 2. See the section "Institutional abbreviation" for details on repositories.

Supplement. The supplement related to this article is available online at: https://doi.org/10.5194/fr-22-91-2019-supplement.

Author contributions. NK did the histological and microanatomical study of long bones and ribs, wrote parts of the manuscript, and prepared figures. AV did the taxonomical assignment of all specimens except for those from the GPI, wrote parts of the manuscript, and prepared figures. HS contributed to the taxonomical assignment of specimens from the GPI collection and to the introduction. TW did the histological study of the vertebrae. JF wrote parts of the manuscript. All authors contributed to the discussion.

Competing interests. The authors declare that they have no conflict of interest.

References

Andrews, R. M.: Patterns of growth in reptiles, in: Biology of the Reptilia. volume 13: physiology D, edited by: Gans, C. and Pough, F. H., Academic Press, London, 273–320, 1982.

Araújo, D. C.: Taxonomy and relation of Proganosauria of basin of Paraná, An. Acad. Bras. Ciênc., 48, 91–116, 1976.

Bickelmann, C. and Tsuji, L. A.: A case study of developmental palaeontology in *Stereosternum tumidum* (Mesosauridae, Parareptilia), Foss. Rec., 21, 109–118, https://doi.org/10.5194/fr-21-109-2018, 2018.

Canoville, A. and Laurin, M.: Evolution of humeral microanatomy and lifestyle in amniotes, and some comments on palaeobiological inferences, Biol. J. Linn. Soc. Lond., 100, 384–406, 2010.

Carroll, R. L.: A short limbed lizard from the *Lystrosaurus* zone (Lower Triassic) of South Africa, J. Paleontol., 56, 183–190, 1982.

Castanet, J., Francillon-Vieillot, H., Meunier, F. J., and de Ricqlès A.: Bone and individual aging, in: Bone volume 7: bone growth, B, edited by: Hall, B. K., CRC Press, Boca Raton, FL, 245–283, 1993.

Chiappe, L. M. and Chinsamy, A.: Pterodaustro's true teeth, Nature, 379, 211–212, 1996.

Cope, E. D.: A contribution to the vertebrate paleontology of Brasil, PAPHS, 25, 7–15, 1886.

Currey, J. D.: Bones: structure and mechanics, Princeton University Press, Princeton, 456, 2002.

de Buffrénil, V. and Mazin, J.-M.: Bone histology of *Claudiosaurus gennniizi* (Reptilia, Claudiosauridae) and the problem of pachyostosis in aquatic tetrapods, Hist. Biol., 2, 311–322, 1989.

de Buffrénil, V., Houssaye, A., and Böhme W.: Bone vascular supply in monitor lizards (Squamata: Varanidae): influence of size, growth, and phylogeny, J. Morphol., 269, 533–543, 2008.

de Ricqlès, A.: Recherches paléohistologiques sur les os longs des tétrapodes V. Cotylosaures et mésosaures, Ann. Paléontol., 60, 171–216, 1974.

de Ricqlès, A. and de Buffrénil, V.: Bone histology, heterochronies, and the return of Tetrapods to life in water: where are we?, in: Secondary Adaptation of Tetrapods to Life in Water: Proceedings of the international meeting, Poitiers, 1996, edited by: Mazin,

J.-M. and de Buffrénil, V., Verlag Dr. Friedrich Pfeil, Munich, Germany, 289–310, 2001.

Du Toit, A. L.: Our wandering continents: an hypothesis of continental drifting, Oliver and Boyd, Edinburgh, 1937.

Francillon-Vieillot, H., Buffrénil de, V., Castanet, J., Géradudie, J., Sire, F. J., Zylberberg, I., and de Ricqlés, A.: Microstructure and mineralization of vertebrate skeletal tissues, in: Skeletal biomineralization: Patterns, Processes and Evolutionary Trends, edited by: Carter, J. G., Van Norstrand Reinhold, New York, 471–530, 1990.

Gervais, P.: Description du Mesosaurus tenudiens. Reptile fossile de l'Afrique australe, Académie des Sciences et Lettres de Montpellier, Mémoires de la Section des Sciences, 6, Teil II, 169–175, 1865.

Houssaye, A.: "Pachyostosis" in aquatic amniotes: a review, Integr. Zool., 4, 325–340, 2009.

Hugi, J. and Sánchez-Villagra, M. R.: Life history and skeletal adaptations in the Galapagos marine iguana (*Amblyrhynchus cristatus*) as reconstructed with bone histological data – a comparative study of iguanines, J. Herpetol., 46, 312–324, 2012.

Hugi, J., Scheyer, T. M., Sander, P. M., Klein, N., and Sánchez-Villagra, M. R.: Long bone microstructure gives new insights into the life of pachypleurosaurids from the Middle Triassic of Monte San Giorgio, Switzerland/Italy, C. R. Palevol., 10, 413–426, 2011.

Karl, H.-V., Gröning, E., and Brauckmann. C.: The Mesosauria in the collections of Göttingen and Clausthal: implications for a modified classification, Clausthaler Geow., 6, 63–78, 2007.

Klein, N.: Long bone histology of Sauropterygia from the Lower Muschelkalk of the Germanic Basin provides unexpected implications for phylogeny, PLoS ONE, 5, e11613, https://doi.org/10.1371/journal.pone.0011613, 2010.

Klein, N. and Griebeler, E. M.: Growth patterns, sexual dimorphism, and maturation modeled in Pachypleurosauria from Middle Triassic of central Europe (Diapsida: Sauropterygia), Foss. Rec., 21, 137–157, https://doi.org/10.5194/fr-21-137-2018, 2018.

Klein, N. and Sander, P. M.: Bone histology and growth of the prosauropod *Plateosaurus engelhardti* Meyer, 1837 from the Norian bonebed of Trossingen (Germany) and Frick (Switzerland), Spec. Pap. Paleontol., 77, 169–206, 2007.

Klein, N., Houssaye, A., Neenan, J. M., and Scheyer, T. M.: Long bone histology and microanatomy of Placodontia (Diapsida: Sauropterygia), Contrib. Zool., 84, 59–84, 2015a.

Klein, N., Neenan, J. M., Scheyer, T. M., and Griebeler, E. M.: Growth patterns and life-history strategies in Placodontia (Diapsida: Sauropterygia), R. Soc. Open Sci., 2, 140440, https://doi.org/10.1098/rsos.140440, 2015b.

Klein, N., Sander, P. M., Krahl, A., Scheyer, T. M., and Houssaye, A.: Diverse aquatic adaptations in *Nothosaurus* spp. (Sauropterygia) – inferences from humeral histology and microanatomy, PLoS ONE, 11, e0158448, https://doi.org/10.1371/journal.pone.0158448, 2016.

Klein, N., Canoville, A., and Houssaye, A.: Microstructure of vertebrae, ribs, and gastralia of Triassic sauropterygians – new insights into the microanatomical processes involved in aquatic adaptations of marine reptiles, Anat. Rec., 302, 1770–1791, https://doi.org/10.1002/ar.24140, 2019.

Konietzko-Meier, D. and Klein, N.: Unique growth pattern of *Metoposaurus diagnosticus* (Amphibia, Temnospondyli) from the Upper Triassic of Krasiejów, Palaeogeogr., Palaeocl., 370, 145–157, 2013.

Laurin, M. and Piñeiro, G. H.: A reassessment of the taxonomic position of mesosaurs, and a surprising phylogeny of early amniotes, Front. Earth Sci., 5, 88, https://doi.org/10.3389/feart.2017.00088, 2017.

Laurin, M. and Reisz, R. R.: A reevaluation of early amniote phylogeny, Zool. J. Linn. Soc., 113, 165–223, 1995.

Lin, K. and Rieppel, O.: Functional morphology and ontogeny of *Keichousaurus hui* (Reptilia, Sauropterygia), Fieldiana Geol., N. S., 39, 1–35, 1998.

MacDougall, M. J., Scott, D., Modesto, S. P., Williams, S. A., and Reisz, R. R.: New material of the reptile *Colobomycter pholeter* (Parareptilia: Lanthanosuchoidea) and the diversity of reptiles during the early Permian (Cisuralian), Zool. J. Linn. Soc., 180, 661–671, 2017.

MacDougall, M. J., Modesto, S. P., Brocklehurst, N., Verrière, A., Reisz, R. R., and Fröbisch, J.: Commentary: A reassessment of the taxonomic position of mesosaurs, and a surprising phylogeny of early amniotes, Front. Earth Sci., 6, 99, https://doi.org/10.3389/feart.2018.00099, 2018.

Modesto, S. P.: Observations on the structure of the Early Permian reptile *Stereosternum tumidum* Cope, Palaeontol. Africa, 35, 7–19, 1999.

Modesto, S. P.: The cranial skeleton of the Early Permian aquatic reptile *Mesosaurus tenuidens*: implications for relationships and palaeobiology, Zool. J. Linn. Soc., 146, 345–368, 2006.

Modesto, S. P.: The postcranial skeleton of the aquatic parareptile *Mesosaurus tenuidens* from the Gondwanan Permian, J. Vertebr. Paleontol., 30, 1378–1395, 2010.

Modesto, S. P. and Anderson, J. S.: The Phylogenetic Definition of Reptilia, Syst. Biol., 53, 815–821, 2004.

Nopcsa, B. F. and Heidsieck, E.: Über eine pachyostotische Rippe aus der Kreide Rügens, Acta Zool., 15, 431–455, 1934.

Núñez Demarco, P. N., Meneghel, M., Laurin, M., and Piñeiro, G.: Was *Mesosaurus* a fully aquatic reptile?, Front. Ecol. Evol., 6, 109, https://doi.org/10.3389/fevo.2018.00109, 2018.

Oelofsen, B. W. and Araújo, D. C.: *Mesosaurus tenuidens* and *Stereosternum tumidum* from the Permian Gondwana of both Southern Africa and South America, S. Afr. J. Sci., 83, 370–372, 1987.

Padian, K. and Lamm, E.-T.: Bone Histology of Fossil Tetrapods: Issues, methods, and databases, University of California Press, Berkeley, 2013.

Piñeiro, G., Ferigolo, J., Meneghel, M., and Laurin, M.: The oldest known amniotic embryos suggest viviparity in mesosaurs, Hist. Biol., 24, 620–630, 2012.

Pretto, F. A., Cabreira, S. F., and Schultz, C. L.: Tooth microstructure of the Early Permian aquatic predator *Stereosternum tumidum*, Acta Palaeontol. Pol., 59, 125–133, 2012.

Romer, A. S.: Osteology of the reptiles, The University of Chicago Press, Chicago, Illinois, 1956.

Rossmann, T. and Maisch, M. W.: Das Mesosaurier-Material in der Bayerischen Staatssammlung für Paläontologie und Historische Geologie: Übersicht und neue Erkenntnisse, Mitt. Bayer. Stslg. Paläontol. Histor. Geol., 39, 69–83, 1999.

Shikama, T. and Ozaki, H.: On a reptilian skeleton from the Palaeozoic formation of San Paulo, Brazil, Trans. Proc. Palaeontol. Soc. Japan, 64, 351–358, 1966.

Skutschas, P. P. and Vitenko D. D.: Early Cretaceous choristoderes (Diapsida, Choristodera) from Siberia, Russia, Cretaceous Res., 77, 79–92, 2017.

Snover, M. L. and Hohn, A. A.: Validation and interpretation of annual skeletal marks in loggerhead (*Caretta caretta*) and Kemp's ridley (*Lepidochelys kempii*) sea turtles, Fishery Bull., 102, 682–692, 2004.

Tsuji, L. A. and Müller, J.: Assembling the history of the Parareptilia: phylogeny, diversification, and a new definition of the clade, Foss. Rec., 12, 71–81, https://doi.org/10.1002/mmng.200800011, 2009.

Villamil, J., Núñez Demarco, P., Meneghel, M., Blanco, R. E., Jones, W., Rinderknecht, A., Laurin, M., and Piñeiro, G.: Optimal swimming speed estimates in the Early Permian mesosaurid *Mesosaurus tenuidens* (Gervais 1865) from Uruguay, Hist. Biol., 28, 963–971, 2016.

Woodward, H. N., Horner, J. R., and Farlow, J. O.: Quantification of intraskeletal histovariability in *Alligator mississippiensis* and implications for vertebrate osteohistology, PeerJ, 2, e422, https://doi.org/10.7717/peerj.422, 2014.